JMEPEG (2011) 20:1491–1496
DOI: 10.1007/s11665-010-9811-1

1059-9495/$19.00

Preform Design for Large-Sized Frame Forging of Ti-Alloy Based on 3-D Electrostatic Field Simulation and Geometric Transformation

Jun Cai, Fuguo Li, and Taiying Liu

(Submitted March 8, 2010; in revised form October 25, 2010)

Large-sized frame forging of Ti-alloy is an important forced component of aircraft. The frame forging has complicated shape which leads to great difficulties in deformation. Some defects may be produced during the forming process such as un-filling or overlapping. Preform design is an effective method for producing qualified forging. In this article, a new method based on 3-D electrostatic field simulation is proposed to design preform of a large-sized frame forging of Ti-alloy and a geometric transformation method is introduced to obtain the preform dimension. In order to select more suitable preform of large-sized frame forging, FEM software Deform-3D is employed to simulate the isothermal forming process of designed preform. Deformation uniformity index ψ is introduced as a criterion to judge the forging quality and the most appropriate preform is obtained by virtual orthogonal test design.

Keywords geometric transformation, large-sized frame forging, preform design, virtual orthogonal experiment, 3-D electrostatic field simulation

1. Introduction

Large-sized frame forging of Ti-alloy is one of the most important forced components of aircraft. These forging parts are used under severe working conditions and required to achieve high geometrical precision and excellent mechanical properties. However, a frame forging has very complex shape which leads to great difficulties in deformation (Ref 1). In the past, forming process and die design of large-sized frame forging were mainly relied on trial and error method. Therefore, the conventional methods, in spite of consume a lot of time and materials, prolonged production time and cannot guarantee forging quality.

Reasonable preform design can improve die filling performance, decrease forming loads, and extend die life. Park et al. (Ref 2) introduced the backward tracing method to design shell noise preform. Fourment and Chenot (Ref 3) proposed an optimization method by optimizing the initial shape of the part and the preform tool during a two-step forging operation. Vazquez and Altan (Ref 4) designed a preform with only 5% material waste by applying changes to the preform geometry and taking advantage of numerical simulation. Srikanth and Zavaras (Ref 5) presented a continuum sensitivity analysis method for the preform design and shape optimization in metal forming. Castro et al. (Ref 6) used genetic algorithms to study preform shape and work-piece temperature. Lee et al. (Ref 7) proposed a method of using equipotential lines and designed the right geometry of preform for a symmetrical disc. On the basis of the minimum energy and the minimum resistance pressure theory, Li (Ref 8) and Wang (Ref 9) demonstrated its feasibility. This method was mostly used under the two-dimension condition, such as symmetrical part (Ref 7, 9, 10) or gas pressure superplastic bulging of sheet (Ref 8). Figure 1 illustrates traditional preform design method based on electrostatic field. The initial shape (billet) is enlarged sufficiently and the final shape (forging) is located inside the initial shape. Then, the voltages of 0 and 1 are applied to the forging and the billet, respectively, and the preform shape is determined among the equipotential lines obtained between the initial and the final shape. However, the equipotential lines are located outside of forging which leads to great difficulties to obtain the actual perform dimension. For example, Wang et al. (Ref 8) divided a P/M super alloy disk into three parts: wheel disk, wheel rim, and hub. Then six equipotential lines close to the final forging shape were chosen as the perform contours. The actual dimension of each part was obtained by reducing the size in accordance with certain proportion after determining the ratio of height to diameter of the preform and then combined into a whole preform. Meanwhile, it is very hard to use traditional approach of electrostatic field to design the preform of non-axisymmetric forging.

The main purpose of this study is proposed a new method based on 3-D electrostatic field simulation to design preform of a large-sized frame forging of Ti-6Al-4V alloy. The forging shape (not enlarged) and the billet shape are separated for a certain distance and combined into a configuration. Then, the voltage of 0 is applied to the forging and outside surface, and voltage of 1 is applied to the billet. Therefore, the preform shape can be regarded as the equipotential fields located inside of the forging shape and the actual preform dimension can be obtained by geometric transformation method conveniently.

Jun Cai, Fuguo Li, and **Taiying Liu**, School of Materials Science and Engineering, Northwestern Polytechnical University, Xi'an 710072, China. Contact e-mail: jeffreycai0116@gmail.com.

2. 3-D Electrostatic Field Simulation of Large-Sized Frame Forging

The frame forging is a complex multi-rib component (Fig. 2) and includes two parts: lug and body. The forging weight is about 90.5 kg, the width of frame body is 150 mm, the maximum length is about 1900 mm, and the minimum rib height is about 50 mm.

2.1 Establishment of 3-D Electrostatic Field Model

The frame forging can be divided into two parts along die parting surface: upper part and lower part. The preform shape of each part is designed independently by 3-D electrostatic field simulation.

The initial billet is a bend bar with elliptical section (a = 65 mm, b = 30 mm). Existing studies have shown that the size of initial shape is not a critical problem because reasonable equipotential lines can be found by choosing an appropriate potential value (Ref 7, 9). Therefore, actual billet size is used as initial shape. Half of the forging is taken as a case to establish 3-D electrostatic field model because of its bilateral symmetry structure.

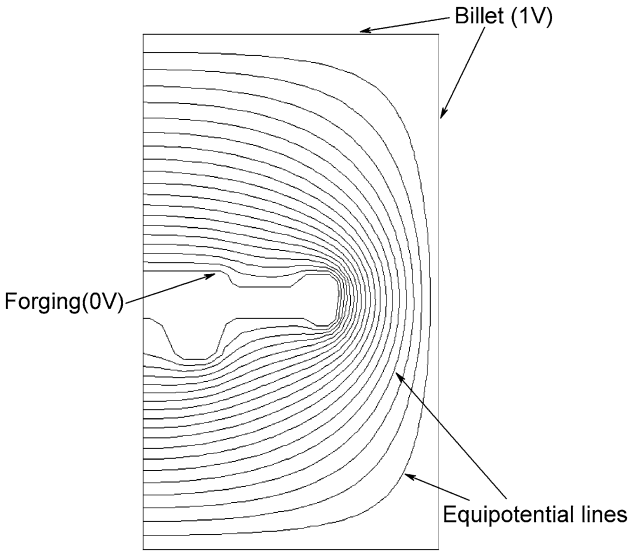

Fig. 1 Traditional method of preform design based on electrostatic field

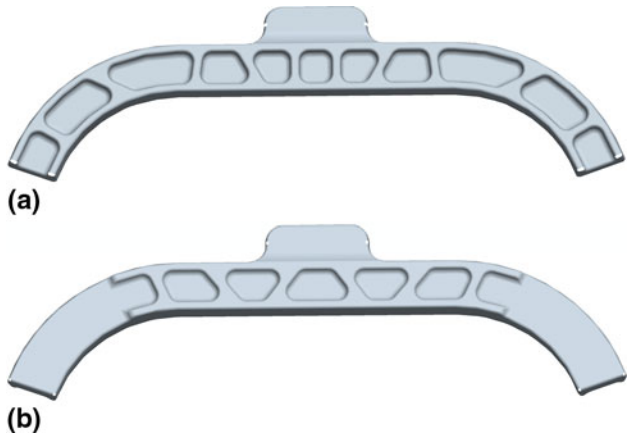

Fig. 2 Geometrical model of large-sized frame forging of Ti-alloy (a) front side and (b) back side

In order to generate suitable electric field, billet and forging are separated for some distance (100 mm in this study). Then the initial shape and the final shape are combined into a configuration, as shown in Fig. 3. The voltage of 1 is applied to the initial shape, and the voltage of 0 is applied to the final shape and the outside surface (Fig. 3a). Therefore, equipotential fields locate between billet and forging (Fig. 3b). Each equipotential line can be regarded as a preform shape, and the actual preform dimension can be obtained by geometric transformation approach.

2.2 Geometric Transformation Approach

Section A-A in Fig. 3(b) is taken as the case to describe the process of geometric transformation. Distribution of equipotential lines of section A-A is shown in Fig. 4. It can be seen form Fig. 4 that the shapes of equipotential lines are too flat and not suitable to be the preform profile when the voltage is higher than 0.15 V. Therefore, the voltages of the equipotential lines should be within in 0.15 V. Frame forging can be regarded as a solid whose section areas have been known, and its volume can be expressed as Eq 1:

$$V \approx \int_0^l A(L)dL, \qquad \text{(Eq 1)}$$

where A is the section area and L is the frame length. For net or near-net forming, section areas of preform should be equal to final forging:

$$A_{\text{preform}} = A_{\text{forging}} \qquad \text{(Eq 2)}$$

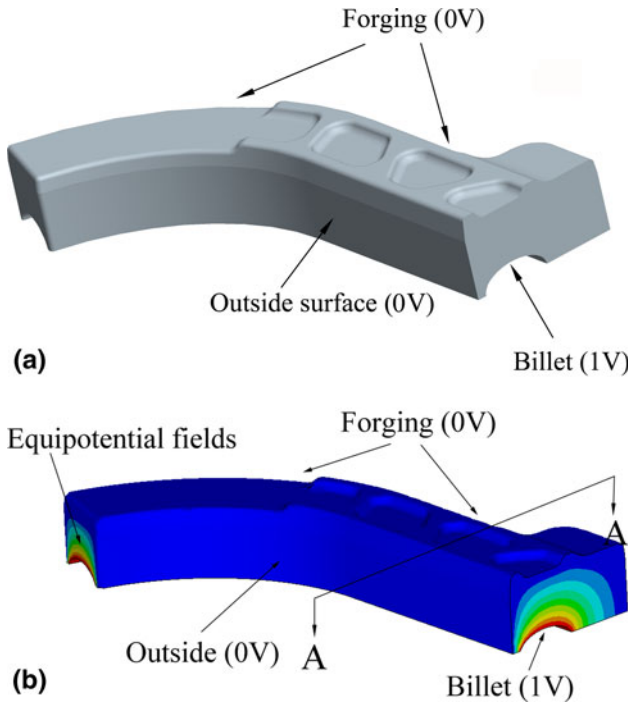

Fig. 3 Geometrical graphs of 3-D electrostatic field simulation. (a) Schematic drawing of 3-D electrostatic field simulation for upper part and (b) electrostatic field distribution of upper part

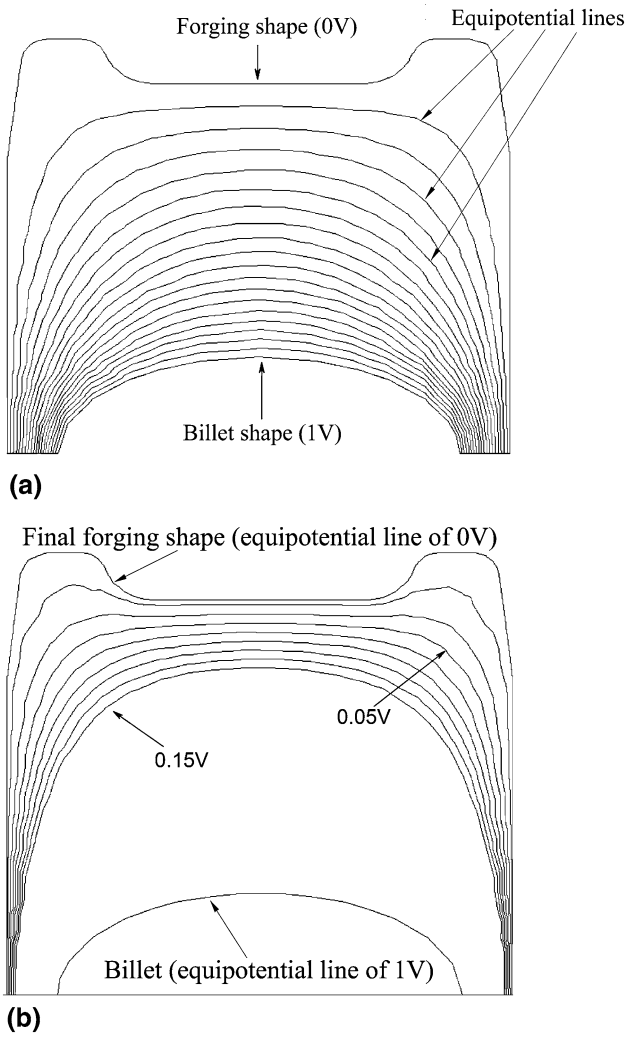

Fig. 4 Electrostatic field distribution of Section A-A (a) 0-1 V and (b) 0.001-0.15 V

For non-precise forging, some section areas of preform should be increased as flash. Then A_{preform} can be described by Eq 3:

$$A_{\text{preform}} = A_{\text{forging}} + A_{\text{flash}} = mA_{\text{forging}}, \quad \text{(Eq 3)}$$

where m ($m > 1$) is a constant, whose value is determined by flash volume. For frame forging, the ribs volume accounts for as much as 12% of total volume, then:

$$A_{\text{preform}} = A_{\text{forging}} + A_{\text{rib}} + A_{\text{flash}} = mA_{\text{forging}} \quad \text{(Eq 4)}$$

There is usually much flash (material waste) in manufacturing flame forging, the goal of this study is to design a preform with about 10% flash that gives complete die fill. Therefore, $m = 1.22$ in this study. The major diameter of ellipse is considered as y axis and minor diameter as x axis. As shown in Fig. 5, ellipse center is chosen to be origin, so the endpoints coordinates of the major diameter N_1 and minor diameter N_2 can be regarded as (a, 0) and (0, b), respectively. Therefore, the coordinate (y, z) of equipotential lines in this coordinate system can be obtained and modeled in CAD software conveniently. Original coordinate of an equipotential line point can be described as [y, z, 1], and

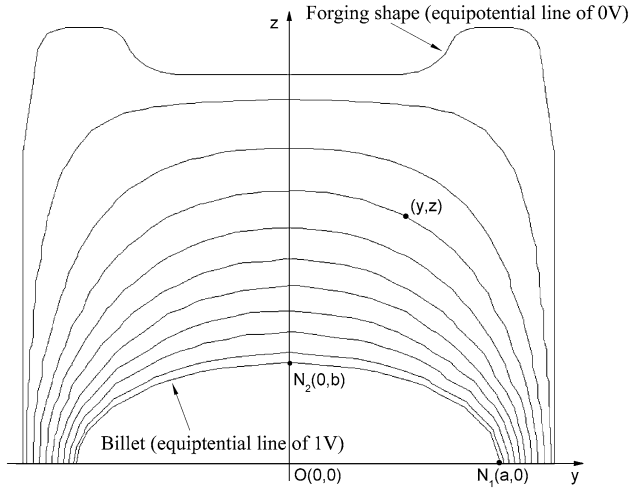

Fig. 5 Establishment of coordinate system

corresponding coordinate [y^*, z^*, 1] of actual preform can be estimated by Eq 5:

$$[y^*, z^*, 1] = [y, z, 1] \cdot T = [y, z, 1] \cdot \begin{bmatrix} a_{11}, a_{12}, a_{13} \\ a_{21}, a_{22}, a_{23} \\ a_{31}, a_{32}, a_{33} \end{bmatrix}, \quad \text{(Eq 5)}$$

where T is called transformation matrix which can be divided into four sub-matrices: $\begin{bmatrix} a_{11}, a_{12} \\ a_{21}, a_{22} \end{bmatrix}$ is scaling and rotation matrix, $[a_{31}, a_{32}]$ is translation matrix, $[a_{13}, a_{23}]^T$ is projection matrix, and $[a_{33}]$ is expansion matrix. For a specific section such as Section A-A, the geometric transformation can be regarded as a 2-D transformation. Therefore, Eq 5 can be simplified as following formula:

$$[y^*, z^*, 1] = [y, z, 1] \cdot \begin{bmatrix} S_y, 0, 0 \\ 0, S_z, 0 \\ 0, T_z, 1 \end{bmatrix} \quad \text{(Eq 6)}$$

where $\begin{bmatrix} S_y, 0 \\ 0, S_z \end{bmatrix}$ is scaling matrix, and $[0, T_z, 1]$ is translation matrix. S_y and S_z are scaling parameters, and T_z is translation vector (translated distance). The area A_{T} closed by equipotential line after translation and y axis can be expressed by following equation:

$$A_{\text{T}} = A_{\text{preform}} = A_{\text{forging}} + A_{\text{rib}} + A_{\text{flash}} = mA_{\text{forging}} \quad \text{(Eq 7)}$$

Afterward, the equipotential line should be scaled because the width of equipotential line after translation is too close to final forging, and scaling parameters should satisfy Eq 8:

$$S_y = \frac{L_{\text{pf}}}{L_{\text{eq}}} = \frac{1}{S_z} \quad \text{(Eq 8)}$$

where L_{pf} is preform width (120 mm in this research), and L_{eq} is width of equipotential line after translation. Figure 6 shows geometric transformation process of 0.05 V equipotential line of Section A-A. Therefore, a series of preforms can be obtained among equipotential fields at varied voltages.

The preforms can be classified into two kinds: the first kind is obtained from equipotential fields at higher voltages. It has a

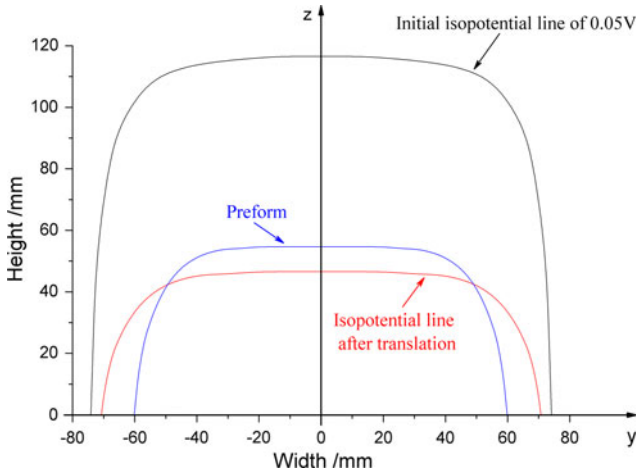

Fig. 6 Geometric transformation of 0.05 V equipotential line at Section A-A

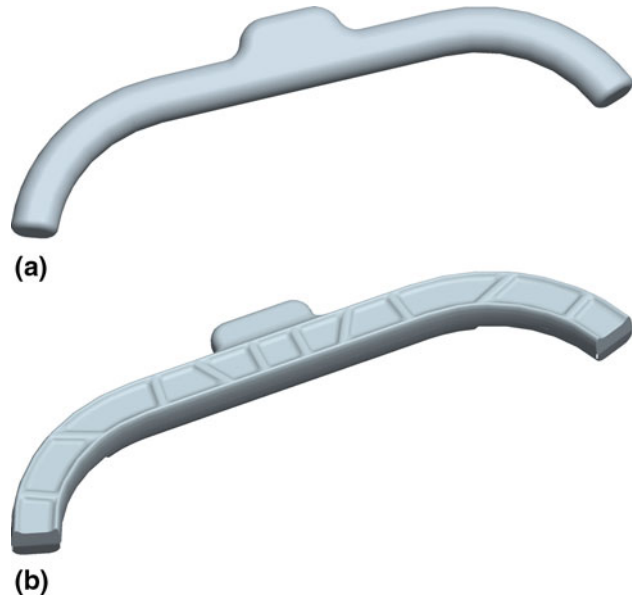

Fig. 7 Preforms designed by 3-D electrostatic field simulation. (a) Preform designed by 0.05 V equipotential field and (b) preform designed by 0.02 V equipotential field

sampler shape which is more close to that of origin billet (shown in Fig. 7a). It is well suitable for the forging that is hard to apply pre-forging process. The second kind is obtained from equipotential fields at lower voltages. It has a more complex shape which is more close to that of final forging. It is suitable for net or near-net forming (shown in Fig. 7b) (Ref 8-10). For frame forging, it would increase too much cost to produce pre-forging dies. Hence, the first kind of preform is used for frame forging.

3. Optimal Selection of Preform Shape

In order to get reasonable preform shape, the frame forging is divided into three regions: lug (region 1), upper body (region 2), and lower body (region 3). As discussed in Sect. 2, equipotential lines should be selected in the voltage range of 0.05-0.15 V. Figure 8 illustrates the electrostatic field distribution of Section A-A ranging from 0.05 to 0.015 V. From Fig. 8, it can be seen that equipotential lines at adjacent voltages show the similar shapes, such as 0.06 and 0.07 V. Meanwhile, choosing too much voltage would result in a significant increase of the computing time. Therefore, equipotential lines at 0.06, 0.09, and 0.12 V are chosen as the preform shape of each region, as shown in Fig. 8. The preform design of frame forging can be regarded as an optimized design problem of multi-factor, so that orthogonal experiment is suitable to select the most suitable factors. FEM software Deform-3D is used to simulate the forming process of designed preforms. During the simulation process, each finite element computation can be regarded as an experiment and the most important factors and how to match factors can be determined by virtual orthogonal experiments.

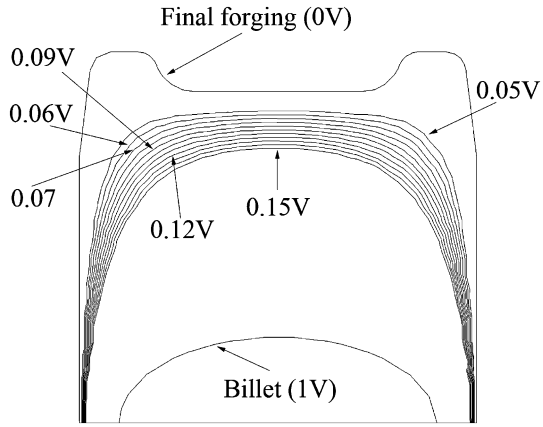

Fig. 8 Electrostatic field distribution of Section A-A: 0.05-0.015 V

$L_9(3^3)$ orthogonal test design (i.e., 9 runs with 3 levels and 3 factors) is constructed to frame forging. The forming temperature is chosen as 920 °C. The workpiece material is Ti-6Al-4V alloy. The upper die velocity is taken to be 1 mm/s, with the lower die remaining stationary. The friction coefficient is taken to be 0.30 for the simulations (Ref 11-13). The constitutive relationship of the Ti-6Al-4V alloy is shown as follows (Ref 14):

$$\sigma = \sigma_0 \cdot f_T \cdot f_{\dot{\varepsilon}} \cdot f_{\varepsilon} \quad \text{(Eq 9)}$$

$$f_T = (-9.79965 \times 10^{-8})T^3 + (2.87618 \times 10^{-4})T^2 - 0.28289T + 93.4123$$

$$f_{\dot{\varepsilon}} = \exp(1.8213 + 0.26366 \ln \dot{\varepsilon})$$

$$f_{\varepsilon} = -2.96246\varepsilon^3 + 4.23111\varepsilon^2 - 2.19419\varepsilon + 1.18007$$

where σ_0 is the initial yield stress (80.47 MPa); f_T, $f_{\dot{\varepsilon}}$, and f are functions of temperature (K), strain rate (s^{-1}), and strain, respectively.In preform design, the main emphasis is on the complete die fill criteria. Furthermore, quality forgings require a more uniform strain distribution throughout the forged part (Ref 15). Therefore, the strain distribution index ψ is introduced to describe the deformation uniformity:

$$\psi = \frac{1}{N}\sum_{i=1}^{N}(\bar{\varepsilon}_i - \bar{\varepsilon}_{\text{avg}})^2 \quad \text{(Eq 10)}$$

Table 1 Three factors (0.06, 0.09, and 0.12 V) at three levels (1, 2, and 3) orthogonal experiment project and results

Test number	Region 1	Region 2	Region 3	ψ	Deformation load, $\times 10^8$ N
1	1 (0.06 V)	1 (0.06 V)	1 (0.06 V)	0.24942	2.26
2	1 (0.06 V)	2 (0.09 V)	2 (0.09 V)	0.30026	1.88
3	**1 (0.06 V)**	**3 (0.12 V)**	**3 (0.12 V)**	**0.20389**	**1.95**
4	2 (0.09 V)	1 (0.06 V)	2 (0.09 V)	0.24502	2.17
5	2 (0.09 V)	2 (0.09 V)	3 (0.12 V)	0.29711	1.95
6	2 (0.09 V)	3 (0.12 V)	1 (0.06 V)	0.29697	1.99
7	3 (0.12 V)	1 (0.06 V)	3 (0.12 V)	0.27866	2.07
8	3 (0.12 V)	2 (0.09 V)	1 (0.06 V)	0.28460	1.94
9	3 (0.12 V)	3 (0.12 V)	2 (0.09 V)	0.23485	1.86
k_1	**0.75357**	0.77310	0.83099		
k_2	0.83910	0.88197	0.78013		
k_3	0.79811	**0.73571**	**0.77966**		
R	0.08553	0.14626	0.05133		

The bold values show the selected equipotential lines

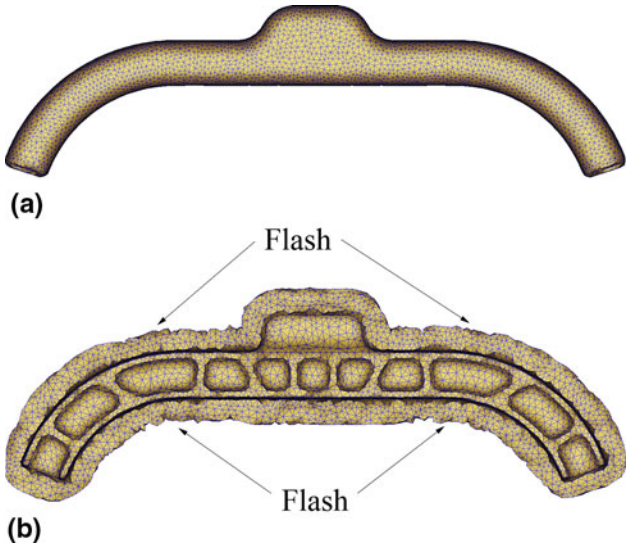

Fig. 9 FEM meshes of (a) preform and (b) forging

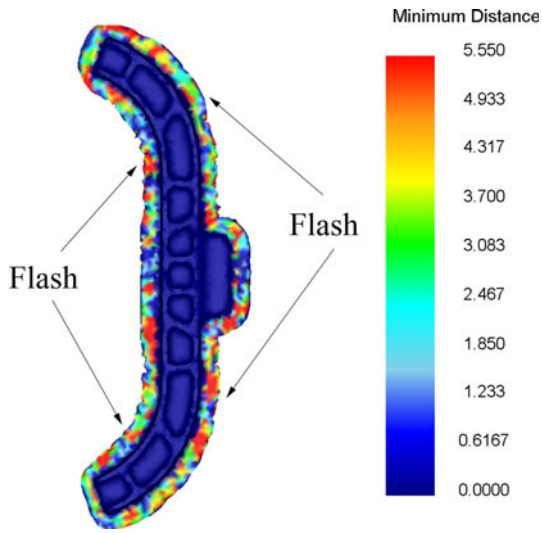

Fig. 10 Minimum distance between die and workpiece (mm)

$$\bar{\varepsilon}_{\text{avg}} = \frac{1}{N}\sum_{j=1}^{N}\bar{\varepsilon}_j$$

where $\bar{\varepsilon}_i$ is the effective strain of an element, $\bar{\varepsilon}_{\text{avg}}$ is the average stain of all elements, and N is the element number. The virtual orthogonal experiment project and results are shown in Table 1. According to the experimental results, the preform shape of region 2 and region 3 have the greatest and least influence on strain distribution, respectively. It also can be seen from Table 1 that 0.06, 0.12, and 0.12 V equipotential lines should be chosen as the preform shape of region 1, region 2, and region 3, respectively. Preform was designed as shown in Fig. 9(a) and the result of finite element analysis is shown in Fig. 9(b). Figure 10 illustrates the minimum distance between the workpiece formed by selected preform and die cavity. It can be seen from Fig. 9(b) and 10 that the die cavity has been completely filled with material (min distance = 0), and the un-filling parts are all located at flash (min distance >0).

4. Conclusion

The following points are derived as the important achievements of the research:

1. A new method based on 3-D electrostatic field simulation is proposed in this study. In order to determine the actual preform dimension, geometric transformation has been introduced. This method of preform design has been shown to be useful and effective for the practical application.
2. Section areas changing can be used to design preform for non-axisymmetric forging. Section areas of preform should be equal to forging for net or near-net forming, while some areas should be increased as flash for non-precise forging.
3. Reasonable preform has been obtained by virtual orthogonal experiment. 0.06, 0.12, and 0.12 V equipotential lines are chosen as the preform shape of lug (region) 1, upper body (region 2), and lower body (region 3),

respectively. FEM simulation results show that the die cavity can be completely filled using the selected preform.

References

1. N.G. Sun, H. Yang, and Z.C. Sun, Optimization on the Process of Large Titanium Bulkhead Isothermal Closed-Die Forging, *Rare Met. Mater. Eng.*, 2009, **38**(7), p 1296–1300
2. J.J. Park, N. Rebelo, and S. Kobayashi, New Approach to Preform Design in Metal Forming with the Finite Element Method, *Int. J. Mach. Tool Des. Res.*, 1983, **23**(1), p 71–79
3. L. Fourment and J.L. Chenot, Optimal Design for Non-steady-state Metal Forming Processes—I. Shape Optimization Method, *Int. J. Numer. Methods Eng.*, 1996, **39**(1), p 33–50
4. V. Vazquez and T. Altan, Die Design for Flashless Forging of Complex Parts, *J. Mater. Process. Technol.*, 2000, **98**(1), p 81–89
5. A. Srikanth and N. Zavaras, Shape Optimization and Preform Design in Metal Forming Processes, *Comput. Methods Appl. Mech. Eng.*, 2000, **190**(13–14), p 1859–1901
6. C.F. Castro, C.A.C. Anotonio, and L.C. Sousa, Optimisation of Shape and Process Parameters in Metal Forging Using Genetic Algorithms, *J. Mater. Process. Technol.*, 2004, **146**(3), p 356–364
7. S.R. Lee, Y.K. Le, C.H. Park et al., A New Method of Preform Design in Hot Forging by Using Electric Field Theory, *Int. J. Mech. Sci.*, 2002, **44**(4), p 773–792
8. C. Li, F.G. Li, Y. Zhang et al., Reverse Educing Method of Bulge-blank Based on Equipotential field, *Jixie Gongcheng Xuebao.*, 2005, **41**(11), p 127–133
9. X.N. Wang and F.G. Li, A Quasi-equipotential Field Simulation for Preform Design of P/M Superalloy Disk, *Chin. J. Aeronaut.*, 2009, **22**(1), p 81–86
10. X.N. Wang, F.G. Li, J. Xiao et al., Preform Design and Finite Element Simulation of New-type P/M Superalloy Disk based on Equipotential Field, *Jixie Gongcheng Xuebao.*, 2009, **45**(5), p 237–243
11. B.S. Kang, J.H. Lee, and S. Kobayashi, Superplastic Forging Design of a Jet Engine Disk by the Finite Element Method, *Int. J. Mach. Tools Manuf.*, 1995, **35**(10), p 1411–1424
12. H. Yang, M. Zhan, and Y.L. Liu, A 3D Rigid-viscoplastic FEM Simulation of the Isothermal Precision Forging of a Blade with a Damper Platform, *J. Mater. Process. Technol.*, 2002, **22**(1), p 45–50
13. H. Kakimoto, T. Arikawa, T. Yoichi et al., Development of Forging Process Design to Close Internal Voids, *J. Mater. Process. Technol.*, 2010, **210**(3), p 415–422
14. N. Lei, F.G. Li, and Y. Fang, New Constitutive Equation Based on Parallel Model for Ti-6Al-4V Alloy, *Hangkong Xuebao.*, 2002, **23**(2), p 190–192
15. N. Thiyagarajan and R.V. Grandhi, Multi-level Design Process for 3-D Preform Shape Optimization in Metal Forming, *J. Mater. Process. Technol.*, 2005, **170**(1–2), p 421–429